Cognitive Neurodynamics (2023) 17:921–940
https://doi.org/10.1007/s11571-022-09876-1

RESEARCH ARTICLE

EEG-based functional connectivity for tactile roughness discrimination

Tahereh Taleei[1] · Mohammad-Reza Nazem-Zadeh[2,3] · Mahmood Amiri[4] · Georgios A. Keliris[5]

Received: 3 February 2022 / Revised: 26 July 2022 / Accepted: 13 August 2022 / Published online: 26 September 2022

Abstract

Tactile sensation and perception involve cooperation between different parts of the brain. Roughness discrimination is an important phase of texture recognition. In this study, we investigated how different roughness levels would influence the brain network characteristics. We recorded EEG signals from nine right-handed healthy subjects who underwent touching three surfaces with different levels of roughness. The experiment was separately repeated in 108 trials for each hand for both static and dynamic touch. For estimation of the functional connectivity between brain regions, the phase lag index method was employed. Frequency-specific connectivity patterns were observed in the ipsilateral and contralateral hemispheres to the hand of interest, for delta, theta, alpha, and beta frequency bands under the study. A number of connections were identified to be in charge of discrimination between surfaces in both alpha and beta frequency bands for the left hand in static touch and for the right hand in dynamic touch. In addition, common connections were determined in both hands for all three roughness in alpha band for static touch and in theta band for dynamic touch. The common connections were identified for the smooth surface in beta band for static touch and in delta and alpha bands for dynamic touch. As observed for static touch in alpha band and for dynamic touch in theta band, the number of common connections between the two hands was decreased by increasing the surface roughness. The results of this research would extend the current knowledge about tactile information processing in the brain.

Keywords Tactile sensation · Functional connectivity · EEG · Roughness discrimination · Static and dynamic touch

Introduction

Touch sense plays a necessary role in human interactions with the external and surrounding environments. There is a complex procedure behind the tactile sensation, from the mechanoreceptors under the skin, to the cortical activities in the brain. The sense of touch enables extracting various information about objects, including identity and material properties such as texture (Ding et al. 2017; Muñoz et al. 2014). When human fingertips touch an object, it produces compression and mechanical deformation, which can stimulate the skin's mechanoreceptors to produce action potentials (Tiwana et al. 2012). The firing rate of the Merkel cell-neurite complex (MCNC) neural network increases with the number of slowly adapting type I (SAI) mechanoreceptors located at the force application point, where the fingertip was pressed by the same sphere at a constant depth and different positions (Yao and Wang 2019). Another critical concept to comprehend the functional basis of texture encoding in the sense of touch is the propagation of skin vibrations away from the contact site. Mechanical energy originating at finger contact propagates through the entire hand as vibration signals that contain enough information to discriminate between the touched objects during natural interactions with ordinary objects. Manfredi et al. 2014 discovered that the frequency composition of texture-elicited vibrations is informative about texture identity when using coarse and fine textures of

✉ Mahmood Amiri
ma_amiri_bme@yahoo.com

[1] Medical Biology Research Center, Institute of Health Technology, Kermanshah University of Medical Sciences, Kermanshah, Iran

[2] Research Center for Molecular and Cellular Imaging, Advanced Medical Technologies and Equipment Institute (AMTEI), Tehran University of Medical Sciences (TUMS), Tehran, Iran

[3] Medical Physics and Biomedical Engineering Department, Tehran University of Medical Sciences (TUMS), Tehran, Iran

[4] Medical Technology Research Center, Institute of Health Technology, Kermanshah University of Medical Sciences, Kermanshah, Iran

[5] Bio-Imaging Lab, University of Antwerp, Antwerp, Belgium

widely used objects. A loss of tactile sensitivity in the hand can be partly compensated by vibrations propagating to a distant part of the limb. Anesthetized controls and patients who have lost tactile sensitivity in the hand can differentiate textures from vibrations propagating to the wrist and forearm (Ryan et al. 2021).

To interact between humans and the external environment, the biological organs that can sense various stimuli play vital roles. Therefore recent research on skin-like tactile sensors attracts extensive attention (Liu et al. 2020). The motivations for research in tactile sensing technology are primarily to develop robots with the same sense of touch as humans (Tiwana et al. 2012). However, today, other important fields of tactile study are emerging, such as Brain-Computer Interface (BCI) (Ziebell et al. 2020), which require extra attention to the details of tactile perception. Due to some diseases or amputation, a sense of touch would be partially lost deteriorating individual daily lives (Conte et al. 2017; Gaetz et al. 2017; Natsuko et al. 2015; Tavassoli et al. 2016). Realistic prosthetic hands with tactile sensing capability are also quite demanding (Oddo et al. 2017). This highlights the importance of analyzing tactile perception to induce tactile sensation for differentiating textures (Raspopovic et al. 2014). Indeed, understanding how the brain listens and responds to tactile sensory information can speed up the design and development of novel prosthetic devices with sensory feedback and active perception. Subsequently, different brain signaling and imaging modalities have been utilized to promote such understanding. Recently, a study discusses the mechanical characterization of the human fingertip that could be useful for developing models in the design of new cutaneous haptic interfaces (Logozzo et al. 2022).

The sense of touch is also critical for providing information about the primary characteristics of objects, like texture, roughness, and softness. Neural and behavioral studies have shed light on the mechanisms and limitations of our sense of touch in the perception of texture and motion, as well as its role in controlling our hand's movement. Ryan et al. 2021 have discussed the interaction between the geometrical and mechanical characteristics of touched objects. Tactile motion improves the discrimination of fine texture elements, whereas the orientation and the spacing of coarse texture elements affect the perceived direction of motion and speed (Moscatelli et al. 2019). Associated with the tactile sensation, roughness detection and perception facilitate texture recognition. Roughness is a texture feature that requires movement between skin and texture, leading to skin vibration. Until now, several studies have been performed on how the peripheral nervous system (PNS) perceives roughness levels (Ding et al. 2017). Nevertheless, this process in the Central Nervous System (CNS) is not completely known and is still under investigation utilizing available tools such as electroencephalography (EEG). Results of brain imaging studies have demonstrated that the major regions are somatosensory, posterior cingulate, and lateral prefrontal cortex, centroparietal sites, lateroparietal operculum, insula, and supplementary motor area in processing the roughness level of a touched surface (Ballesteros et al. 2009; Kim et al. 2015; Kitada et al. 2005). Additionally, the cortical processing of roughness discrimination follows two schemes, cognitive and sensory-based processing. The former generates an activation in the prefrontal areas, while the latter involves mostly in the somatosensory region (Lederman and Klatzky 2009). Alternations in alpha and beta bands frequency have been observed, indicating that the alpha band energy is linearly reduced as the surface roughness is increased (Genna et al. 2018, 2017). In another study, an involvement of the occipital area during tactile exploration tasks has been suggested. A sensory substitution process is reflected by increasing the local beta 1 power in occipital derivations, as well by increasing the coherence in visuospatial-related derivations (Campus et al. 2012). Moreover, the total power in the mu (8–15 Hz) and beta (16–30 Hz) frequency bands has been demonstrated highly accurate in discriminating textures with different levels of roughness (Eldeeb et al. 2020).

Previous studies of roughness perception have mainly focused on the visualizing and analysis of different brain waves and event-related potentials (ERP). The alternations in the characteristics of other brain sensory networks have been reported for auditory (Mohan et al. 2016), vision (Chai et al. 2017), and brain sensory disorders (Afshari and Jalili 2016; Ala et al. 2018; Rubinov and Sporns 2010). However, original works related to the characteristics in the brain sensory network through touching surfaces are missing.

Various measures, such as phase synchronization index (PSI) (Hurtado et al. 2004), mutual information (Hurtado et al. 2004), and partial directed coherence (Varotto et al. 2012) have been applied for the quantification of functional connectivity among different brain units with multichannel neural signals including EEG. Among these, PSI is used for analyzing the interaction between brain units, especially where the interaction is too weak to detect by other measures. It can effectively quantify the relationship between rhythms, i.e., instantaneous phase (IP) extracted from observed signals, but would neglect the effect of instantaneous amplitude. To detect the level of phase synchronization (PS) in a pair of signals, various definitions of IP have been proposed. When the IP difference of two coupled units (or the IP extracted from a pair of signals) is bounded with respect to time, the coupled units are said to be in PS. The PSI has been widely used in different neuroscience and neurology domains. Some applications are, to quantify the alternation of neuronal synchrony after

focal ischemic stroke, to investigate the spatiotemporal dynamics of cortical connectivity in preictal phases in patients with epilepsy, to classify the mental states in brain—computer interface, and to provide new insights in Parkinson's and Alzheimer's diseases (Sun et al. 2012).

In the present study, the changes of the characteristics in the brain sensory network when subjects are touching surfaces with different levels of roughness is investigated. The aim is to increase our understanding about tactile sensory system's functions and hence the functional connectivity between different brain regions is calculated. It gives a functional connectivity matrix with each element representing the strength of functional connectivity between two brain sources or cortical regions. Specifically, we evaluate the EEG-based functional connectivity for roughness perception using the PSI method, and examine how functional connectivity in different frequency bands is changed when the subject touches surfaces with different roughness. Results show that not only tactile stimulation by the right or left hands triggers different connections but also the roughness level of the surface being touched causes a significantly different response in the brain connections.

Methods

Subjects and data recording

A 32-channel EEG signal was recorded from nine right-handed and healthy subjects (4 females and 5 males, average age 27 $\pm$ 1.5 years). Participants had no history of peripheral neuropathy diseases, skin diseases, or neurological disorders. Before the experiment, the procedure and regulations were fully explained to all participants who signed the informed consent form. The EEG signal was recorded with a sampling rate of 512 HZ. The electrode installation was based on the international 10–20 electrode location system at the Iranian National Brain Mapping Lab (NBML). The protocol was ethically approved by the Iran University of Medical Science (#IR.IUMS.REC.1396.0294) and Kermanshah University of Medical Sciences (#IR.KUMS.REC.1396.729). All methods were performed in accordance with the relevant guidelines and regulations in accordance with the Declaration of Helsinki (Association 2013).

Experimental Setup

Before the experiment, the volunteers sat on a comfortable chair in a relaxing position and place their right-hand index fingertip on a surface mounted on a rotating plate. To prevent unwanted movements, the rest of the fingers were held in place by a holder, while the hand muscles were relaxed (Fig. 1). We placed three surfaces with different levels of roughness on the plate. We designed a microcontroller-based electronic system to control the speed of the rotating plate and its vertical movement as well as the time interval of the rotation. The surface types included a rough (hardness degree: P60), a semi-rough (hardness degree: P100) and a smooth surface (hardness degree: P280). The grit size of the sandpapers is determined based on a European system (Yourself MBHIaDI 2013).

During the experiment, the rotating plate was automatically elevated to touch the subject's fingertip, where the position was held fixed for 2 s (contact situation or static touch). Then, it was automatically turned such that each roughness was pulled out underneath the index fingertip for another 2 s (dynamic touch). Next, the wheeling plate was automatically descended to detach from the fingertip (no contact situation) for another 2 s. Finally, it was rotated to change into the next material. This procedure was repeated. To avoid acclimatization error, we applied two different sequences: rough, smooth, semi-rough; and smooth, rough, semi-rough; each repeated 18 times. In summary, subjects underwent touching each of the three surfaces 36 times during the experiment. The subjects had a short rest (5 min), after which the abovementioned procedure was repeated for the left (non-dominant) hand. The whole procedure for both hands lasted about 30 min. After the whole experiment, no participant declared any complaints including fatigue.

Preprocessing

The raw data was processed using custom-written code for the EEGLAB (Delorme and Makeig 2004) MATLAB toolbox. First, the EEG signal was purified by removing the baseline (detrending) and band pass filtering between 0.5 and 40 Hz. Then, the signal was re-referenced to the channels average signal. Independent Component Analysis (ICA) is a useful method for distinguishing the brain and non-brain activities and removing artifacts (e.g., eye artifacts, muscle artifacts and electrocardiographic activity) from the raw data (Jung et al. 2000). However, it highly depends on the user expertise and thus we also used the ICLabel method to check the obtained components. Our device was synchronized with EEG device and sent appropriate pulses in response to the events. These pulses allowed us to detect and label the events (dynamic touch, static touch, and no touch). Each trial consisted of 9 s. The EEG epochs associated with a 2-s baseline (no contact situation), a 2-s static touch, and a 2-s dynamic touch were segmented. To extract functional connectivity between the channels, the PSI were extracted (Astolfi et al. 2008). In the present study, the phase-lag index (PLI) (a subset of the

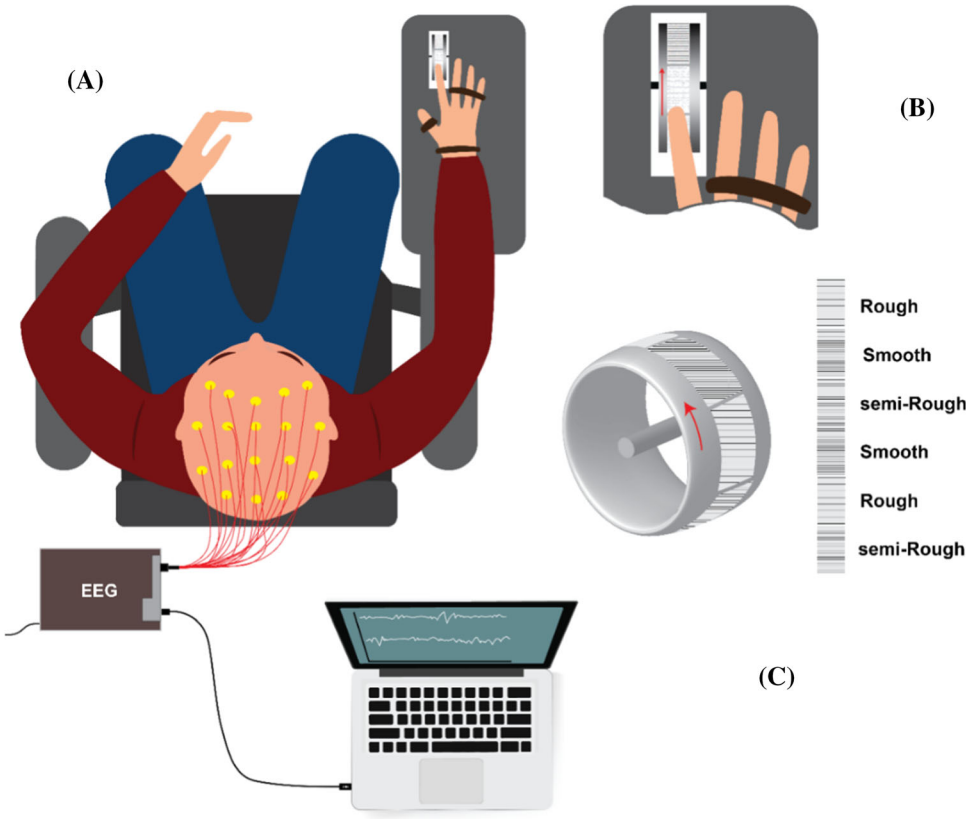

Fig. 1 Schematic of the experiment setup. **A** The subject sits on a comfortable seat with the eyes closed. **B** The subject's index finger is secured over the surface and other fingers are fixed in order to prevent unwanted movements. **C** The rotating plate with different surface roughness. Upon starting the device, the wheeling plate automatically moves up to touch the subject's fingertip, and holds its position for 2 Sec (static touch). Then, it rotates for 2 Sec, during which the subject feels the movement of the material under his/her index fingertip (dynamic touch). Next, the surface automatically moves down to detach from the fingertip for another 2 Secs with no contact (baseline, no contact situation). Finally, it rotates to change into the next material. This procedure is repeated again. During the experiment, an EEG signal is collected from the participant. A total of 108 trials for both right and left index fingers per subject are collected (36 trials for each roughness level)

PSI) was specifically used to estimate the functional connectivity.

Phase synchronization indices

Phase synchronization refers to a situation when the phases of two coupled oscillators get synchronized, even if their amplitudes are uncorrelated (Rosenblum et al. 1996). In the phase-locking condition:

$$\Delta\varnothing(t) = \left|\varnothing_x(t) - \varnothing_y(t)\right| \leq constant \tag{1}$$

$$\varnothing_x(t) = arctg\frac{x_H(t)}{x(t)} \tag{2}$$

In real systems, the signals are often noisy. Hence, one has to work with the cyclic relative phase, which is the relative phase difference wrapped to the interval [0,2π). It is defined as:

$$\Delta\varnothing_{rel}(t) = \Delta\varnothing(t) mod 2\pi \tag{3}$$

Before estimating the degree of phase synchronization between two signals, some pre-processing steps are necessary. First, the corresponding analytic signals $x_{an}(t)$ and $y_{an}(t)$ should be obtained from the real-valued signals x(t) and y(t):

$$x_{an}(t) = x(t) + ix_H(t) = A_x(t)e^{i\varnothing_x(t)} \tag{4}$$

$$y_{an}(t) = y(t) + iy_H(t) = A_y(t)e^{i\varnothing_y(t)} \tag{5}$$

where $x_H(t)$ and $y_H(t)$ are the Hilbert transforms (Hilbert 2009) of x(t) and y(t):

$$x_H(t) = \frac{1}{\pi}P.V.\int_{-\infty}^{\infty}\frac{x(t)}{t-\tau}d\tau \tag{6}$$

where P.V. is the Cauchy's Principal Value. Finally, the instantaneous amplitude and phase of $x_{an}(t)$ are calculated (similar notations for $y_{an}(t)$):

$$A_x(t) = \sqrt{x_H(t)^2 + x(t)^2} \tag{7}$$

Phase-lag index (PLI)

Actual interaction between two neural sources leads to a coherent phase relationship between their corresponding time series. To estimate the functional connectivity measures, we used PLI, which measures the asymmetry in distribution of phase differences between two signals. The main advantage of this method is that it is less sensitive to the volume conduction, the common sources, and the electrode montage. However, it bears some disadvantages including the risk of missing linear yet functionally meaningful interactions and the chance of missing small values under noisy conditions (Stam et al. 2007). The PLI (Stam et al. 2007) discards the phase distributions that are centered around 0 mod π, showing a robust behavior against the common sources (e.g. the volume conduction).

$$PLI = |\langle sign(\Delta\emptyset_{rel}(t))\rangle| = \left|\frac{1}{N}\sum_{n=1}^{N} sign(\Delta\emptyset_{rel}(t_n))\right| \quad (8)$$

N is the number of samples. This index is between 0 and 1. The condition PLI = 0 implies no coupling or coupling with a phase difference centered around 0 mod π, while PLI = 1 suggests a perfect phase locking at a value of $\Delta\varnothing_{rel}(t)$ different from 0 mod π.

Statistical analysis

After preprocessing, a functional connectivity matrix was calculated for each of the three roughness levels including smooth surface (SS), semi-rough surface (SRS), rough surface (RS) for the right hand (RH) and the left hand (LH) in baseline, static and dynamic touch, then the statistical comparisons were performed. The comparisons were made for four frequency bands of delta (δ, 1–4 Hz), theta (θ,4–8 Hz), alpha (α, 8–13 Hz), and beta (β, 13–30 Hz). We first explored the functional connectivity for the right and left hands and for three levels of roughness. Then, we investigated how a functional connectivity is altered as the level of roughness changes for either hand.

SPSS24 and MATLAB statistical analysis were used. One-way analysis of variance (ANOVA) is a parametric test in order to compare the means of more than two groups. This test was applied to investigate the significance of the variations between the functional connectivity for touching surfaces with different roughness. Finally, a Tukey post hoc test was utilized to find the variations within the roughness cohorts. Before performing the statistical analysis, it was ensured that the data maintains a normal distribution. The alpha-error-level for significance was set to the conventionally used α = 0.05. The significance thresholds were adjusted to account for multiple comparisons using the False Discovery Rate (FDR) method (Benjamini 2010).

Results

Delta and theta bands

PLI method in both delta and theta bands did not detect any significant difference between the three roughness levels for either of the hands by static and dynamic touch, after FDR adjustment. The results are illustrated in Figs. S1A, S1B, S1C, S2A, S2B and S2C.

Alpha band

The connectivity pattern for the three levels of roughness (i.e., rough, semi-rough & smooth) by baseline, static and dynamic touch using the PLI method in alpha band is illustrated in Fig. 2A, B, C. For the right hand by static touch, the connections in alpha band for the SS were more than for the two other surfaces. In addition, compared to baseline, the connections for the SS in frontal and prefrontal regions were increased. There was a connection between right temporal (T8) and prefrontal (Fp1) for the RS that was not observed in baseline and dynamic touch. For static touch, there was a connection in alpha band between left frontal (F7) and parietal (PO3) for the smooth and rough surfaces, which was not observed for the semi-rough surface. Moreover, there was a connection in alpha band between left and right central (C3, C4) for the smooth surface that was not observed in baseline and dynamic touch and for the two other surfaces. For dynamic touch, the connections for the RS and SS were decreased compared to static touch, with strong connection between left parietal (P7) and right frontal (F4), and right central (C4) and FC5 for the SS and RS, respectively. For the left hand by static touch, the number of strong connections for the RS was drastically less than the two other surfaces in alpha frequency band. The number of connections between frontal and parietal regions was increased compared to baseline and dynamic touch for the SRS. Furthermore, compared to the baseline, some connections between left temporal (T7) and the frontal region were observed for the SS in static touch.

Figure 3 compares the functional connectivity pattern for three roughness levels in alpha band by static touch (p-value < 0.05, after adjustment for multiple comparisons). For the left hand, a significant connection in alpha band (between central and frontal regions) was seen between the RS and SRS and also, between the SRS and SS, where the connection for the SRS was measured stronger than for two other surfaces. For the right hand, no significant difference

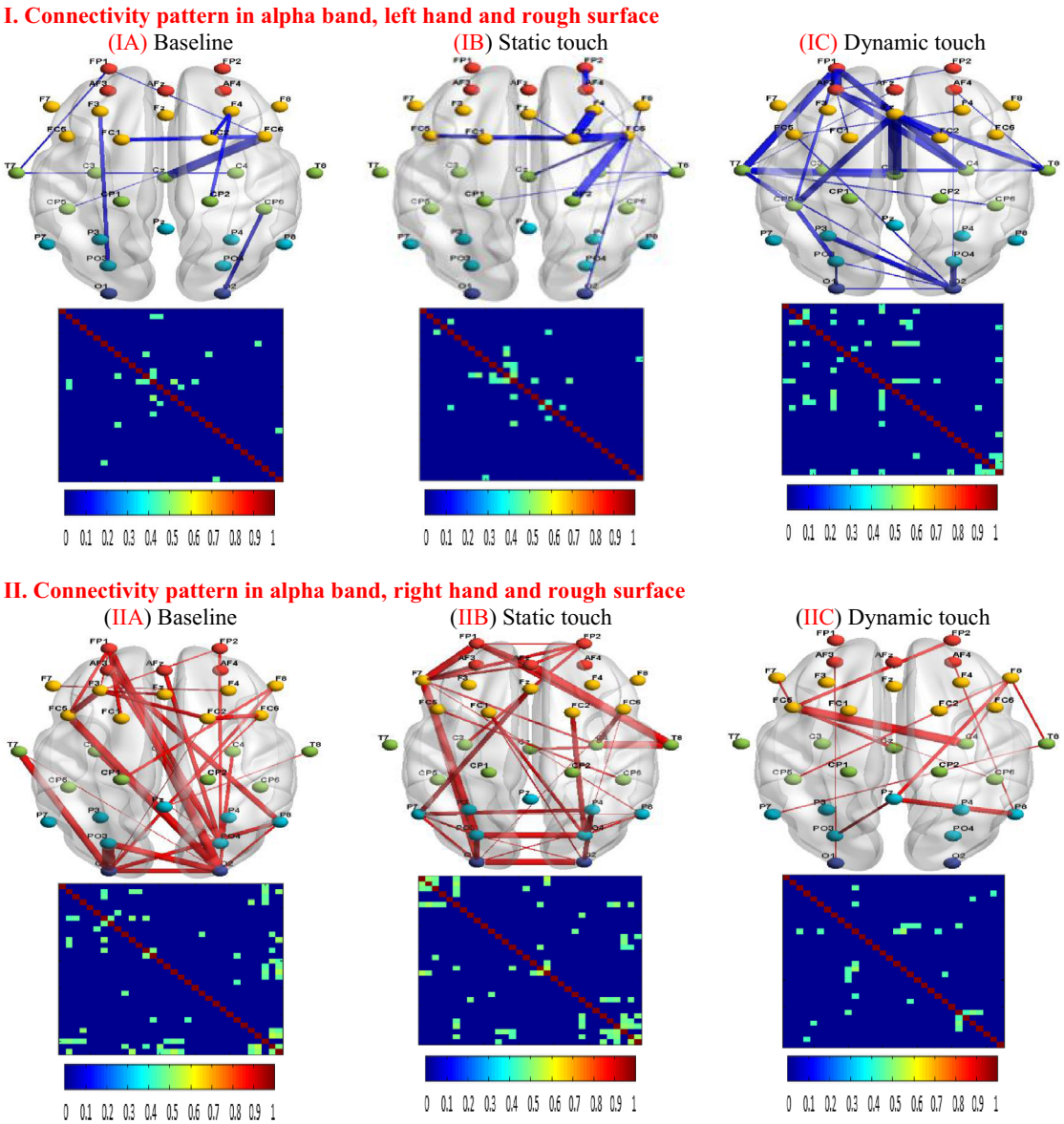

Fig. 2 **A** Connectivity pattern in alpha band using the PLI estimator for RS (IA, IIA), (IB, IIB), (IC, IIC) showing the connectivity matrix and the average connectivity representation for the left and right hands in the baseline, and by static and dynamic touch, respectively. Each color bar indicates the strength of connections for matrices from 0 to 1 (RS: rough surface; blue color: left hand; red color: right hand). **B** Connectivity pattern in alpha band using the PLI estimator for SRS (IIIA, IVA), (IIIB, IVB), (IIIC, IVC) showing the connectivity matrix and the average connectivity representation for the left and right hands in the baseline, and by static and dynamic touch, respectively. Each color bar indicates the strength of connections for matrices from 0 to 1 (SRS: semi-rough surface; blue color: left hand; red color: right hand). **C** Connectivity pattern in alpha band using the PLI estimator for SS (VA, VIA), (VB, VIB), (VC, VIC) showing the connectivity matrix and the average connectivity representation for the left and right hands in the baseline, and by static and dynamic touch, respectively. Each color bar indicates the strength of connections for matrices ranging from 0 to 1 (SS: smooth surface; blue color: left hand; red color: right hand). (Clolor figure online)

was observed in alpha band between the three roughness levels.

Figure 4 compares the functional connectivity patterns for three roughness levels in alpha band by dynamic touch (p-value < 0.05, after adjustment for multiple comparisons). For the right hand, significant variations were observed in three specific connections in alpha band between the RS and SS, the RS and SRS, and also between the SRS and SS, where the connections for the smooth surface were measured weaker than two other surfaces. For the left hand, no significant variation in alpha band was observed between the three roughness levels in functional connections.

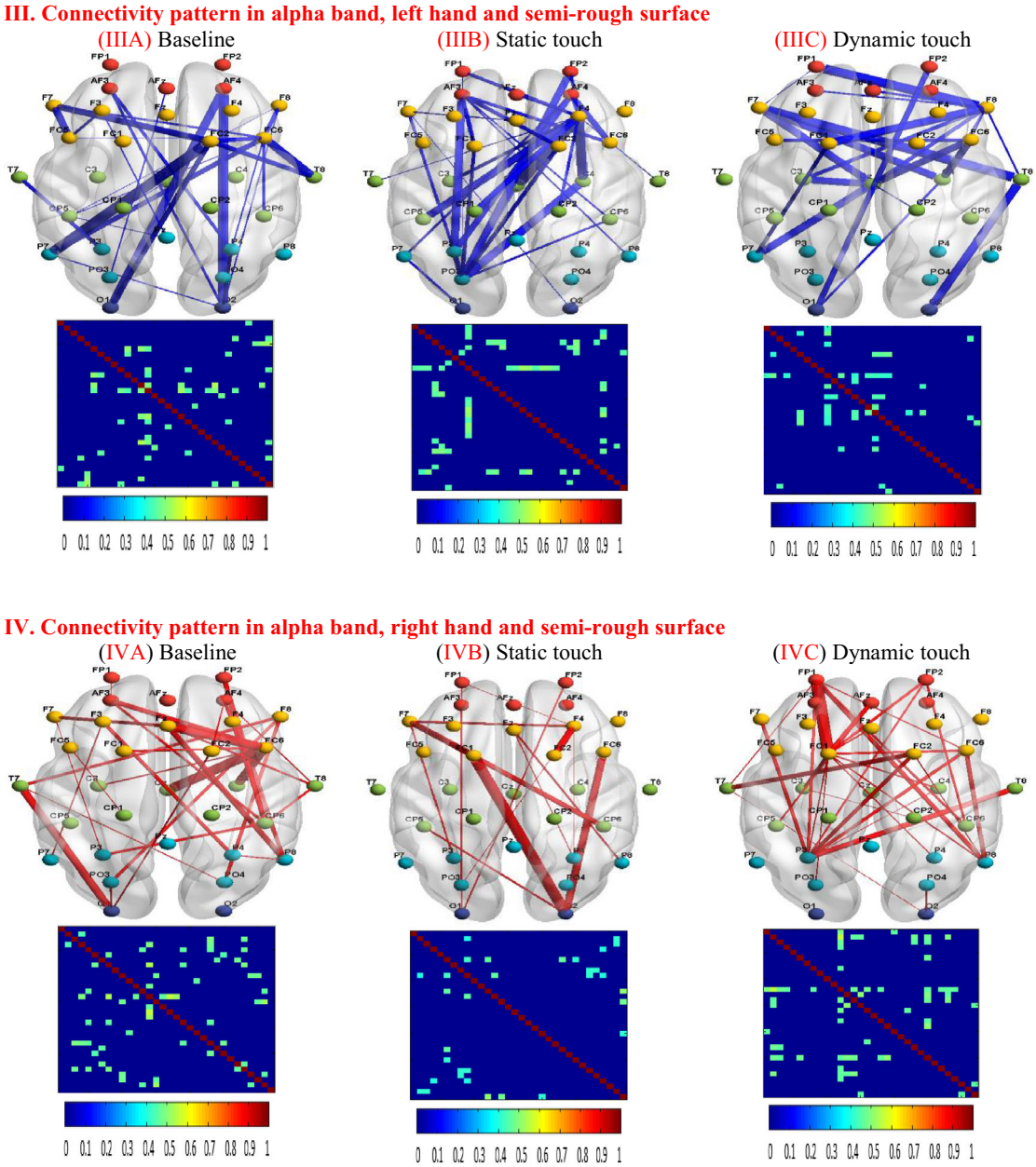

Fig. 2 continued

Beta band

The connectivity pattern for three levels of roughness (i.e., rough, semi-rough & smooth) in baseline, static and dynamic touch using the PLI method in beta band is illustrated in Fig. 5A, B and C. For the right hand by static touch, the number of strong connections in beta band for the SS was reduced compared to the two other surfaces. On the contrary, the number of strong connections in dynamic touch for the SS was increased compared to the two other surfaces, the most connections were concentrated in the frontal and central regions. In addition, the number of connections in beta band in static touch for RS and SS was reduced compared to the baseline. Moreover, the number of strong connections for the SRS in frontal region were created compared to the baseline. Moreover, in dynamic touch compared to the baseline and static touch, the connections for the RS were reduced, mostly centralizing in frontal and central regions. For the left hand in static touch, the connections in beta band were concentrated mainly in frontal regions for the SS compared to the baseline.

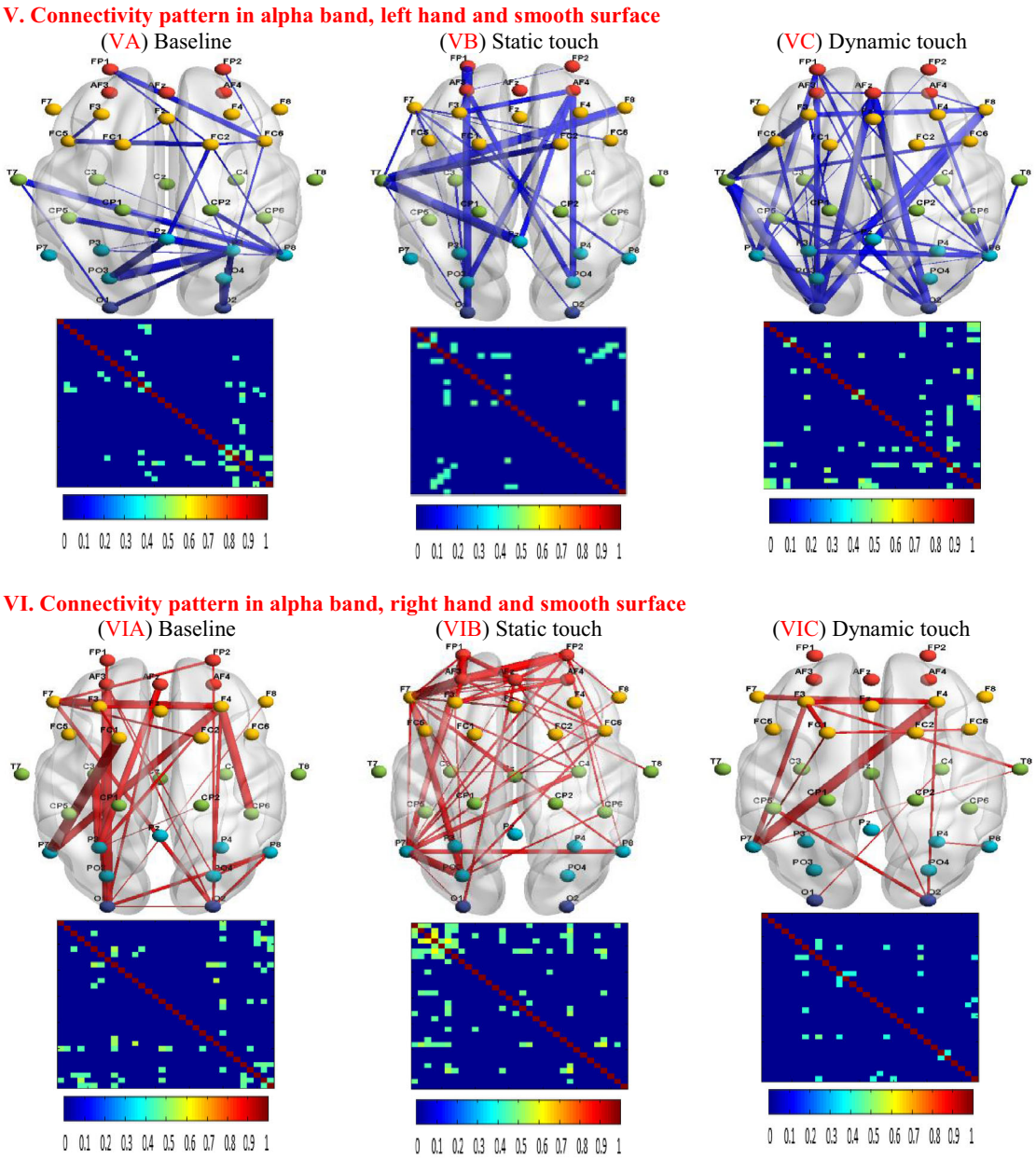

Fig. 2 continued

Furthermore, in dynamic touch compared to the baseline and static touch, the connections for the RS were decreased.

Figure 6 illustrates the results of comparisons between the roughness levels in beta band in static touch (p-value < 0.05, after adjustment for multiple comparisons). For the left hand, significant variations were observed in three specific connections in beta band between the RS and SRS, and also between the SRS and SS. For the right hand, no significant variation in beta band was observed between the three roughness levels in connections.

Figure 7 demonstrates the results of comparisons between the roughness levels in beta band in dynamic touch (p-value < 0.05, after adjustment for multiple comparisons). For the right hand, variations in three specific connections were significant in beta band between the RS and SS, RS and SRS, and also between the SRS and SS. For the left hand, variations in beta band between the three roughness levels in connections were insignificant.

We examined the significant connections between the right and left hands for the different roughness levels, to understand which hand (dominant hand or the other hand) may cause a stronger functional connectivity in the brain

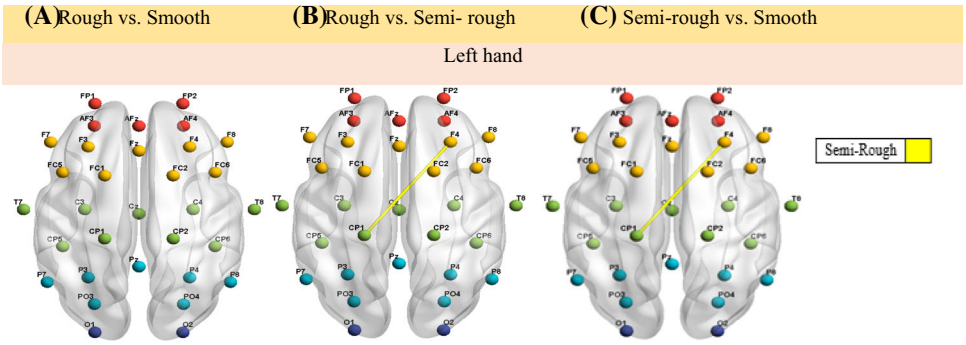

Fig. 3 Significant different (p-value < 0.05) connectivity pattern using the PLI estimator in alpha band between the three roughness levels for the left hand by static touch. **A** No significant difference was observed between RS and SS. **B** Significant differences between RS and SRS: the connection in yellow indicates that the connection for SRS was stronger than RS. **C** Significant differences between SS and SRS: the connection in yellow indicates that SRS was stronger than SS. Note that for the left hand, only one significant connection was seen between SRS and RS and also SRS and SS surfaces, indicating that the connection for LH-SRS is stronger than the other two surfaces. SS: smooth surface, SRS: semi-rough surface, RS: rough surface, RH: right hand, LH: left hand. (Color figure online)

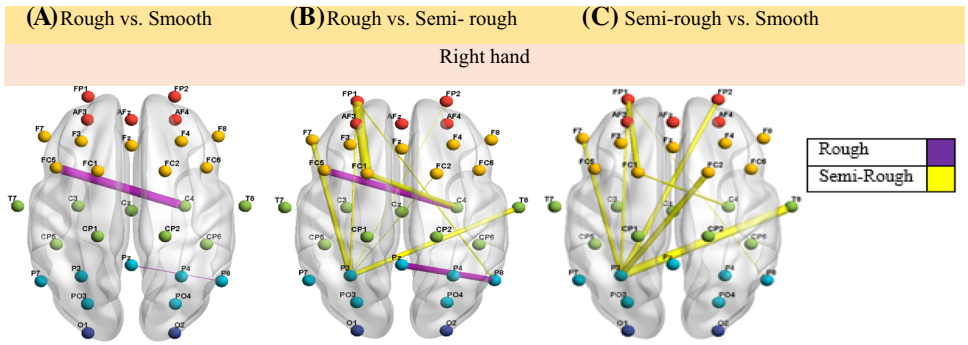

Fig. 4 Significant different (p-value < 0.05) connectivity pattern using the PLI estimator in alpha band between the three roughness levels for the right hand by dynamic touch. **A** Significant differences between RS and SS: the connection in purple indicates that the connection for RS was stronger than SS. **B** Significant differences between RS and SRS: the connection in yellow indicates that the SRS was stronger than the RS and the purple lines represent the opposite case. **C** Significant differences between SS and SRS: the connection in yellow indicates that the SRS was stronger than the SS. Note that for the right hand, the significant differences were seen between the RS and the SS, indicating that the connection for RH-RS is stronger than the RH-SS and in addition, the significant differences were seen between the RS and the SRS and also SRS and SS surfaces, dominant connections indicate that the connections for RH-SRS were stronger than the other two surfaces in the alpha band. SS: smooth surface, SRS: semi-rough surface, RS: rough surface, RH: right hand, LH: left hand. (Color figure online)

according to different levels of roughness. We observed significant connections in static touch between the left and right hands for 1—the SRS in delta band, 2—the RS in alpha band, 3—both SRS and SS in beta band. Also, we observed significant connections in dynamic touch between the left and right hands for 1—the RS in delta band, 2—the SRS in theta band, 3—the SRS in Alpha band (p-value < 0.05, after adjustment for multiple comparisons, Tables 1and 2 and Figs. 8 and 9). There was no significant difference between the right and left hands for any of roughness levels in theta band for static touch and beta band for dynamic touch. A common connection was found between all subjects in the left hand for static touch in theta band for SRS. There was a common connection between right occipital (O2) and right frontal (F8) regions (Fig. 10). Also, common connections were determined between the right and left hands for static touch in alpha band for all roughness levels and in beta band for only the SS and also for dynamic touch in delta band for only SS, in theta band for all roughness levels and in alpha band for only SS (Tables 3 and 4). As observed in alpha band for static touch, the number of common connections between the two hands is decreased by increasing the roughness level. Also, in theta band for dynamic touch, the number of common connections between the two hands is decreased by increasing the roughness level.

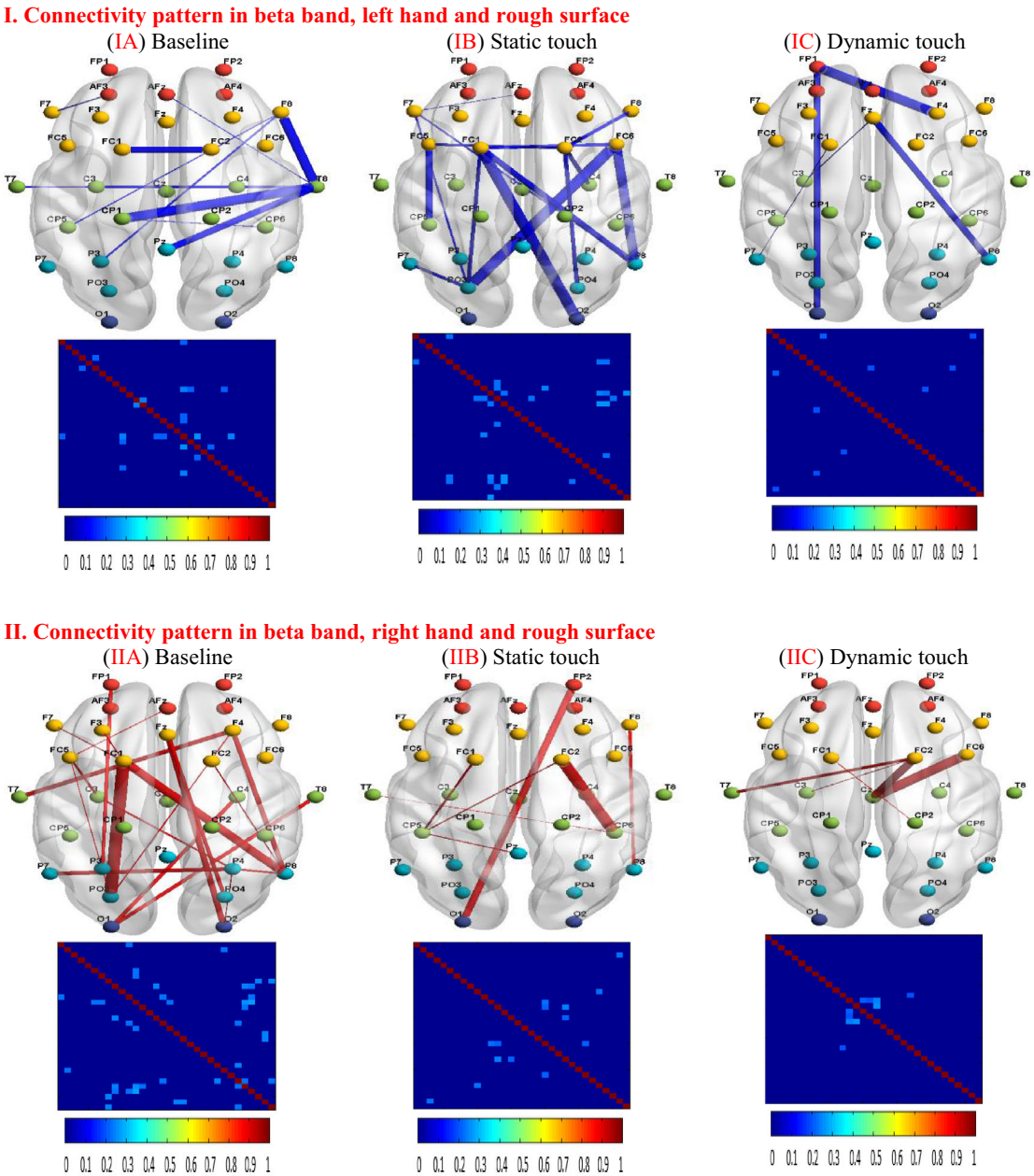

Fig. 5 **A** Connectivity pattern in beta band using the PLI estimator for RS (IA, IIA), (IB, IIB), (IC, IIC) showing the connectivity matrix and the average connectivity representation for the left and right hands in the baseline, and in static and dynamic touch, respectively. Each color bar indicates the strength of connections for matrices from 0 to 1 (RS: rough surface; blue color: left hand; red color: right hand). **B** Connectivity pattern in beta band using the PLI estimator for SRS (IIIA, IVA), (IIIB, IVB), (IIIC, IVC) showing the connectivity matrix and the average connectivity representation for the left and right hands in the baseline, and in static and dynamic touch, respectively. Each color bar indicates the strength of connections for matrices from 0 to 1 (SRS: semi-rough surface; blue color: left hand; red color: right hand). **C** Connectivity pattern in beta band using the PLI estimator for SS (VA, VIA), (VB, VIB), (VC, VIC) showing the connectivity matrix and the average connectivity representation for the left and right hands in the baseline, and in static and dynamic touch, respectively. Each color bar indicates the strength of connections for matrices from 0 to 1 (SS: smooth surface; blue color: left hand; red color: right hand). (Color figure online)

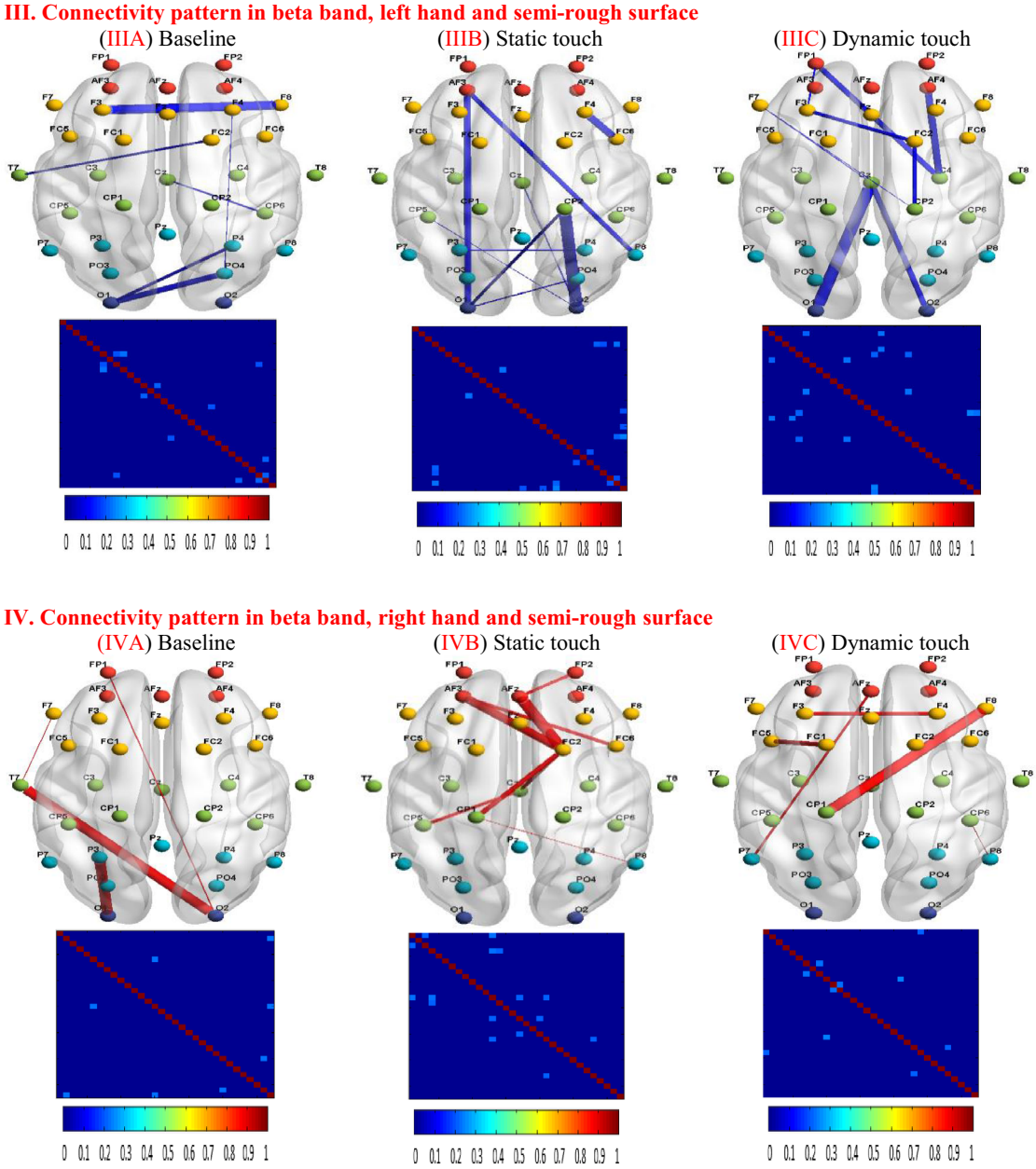

Fig. 5 continued

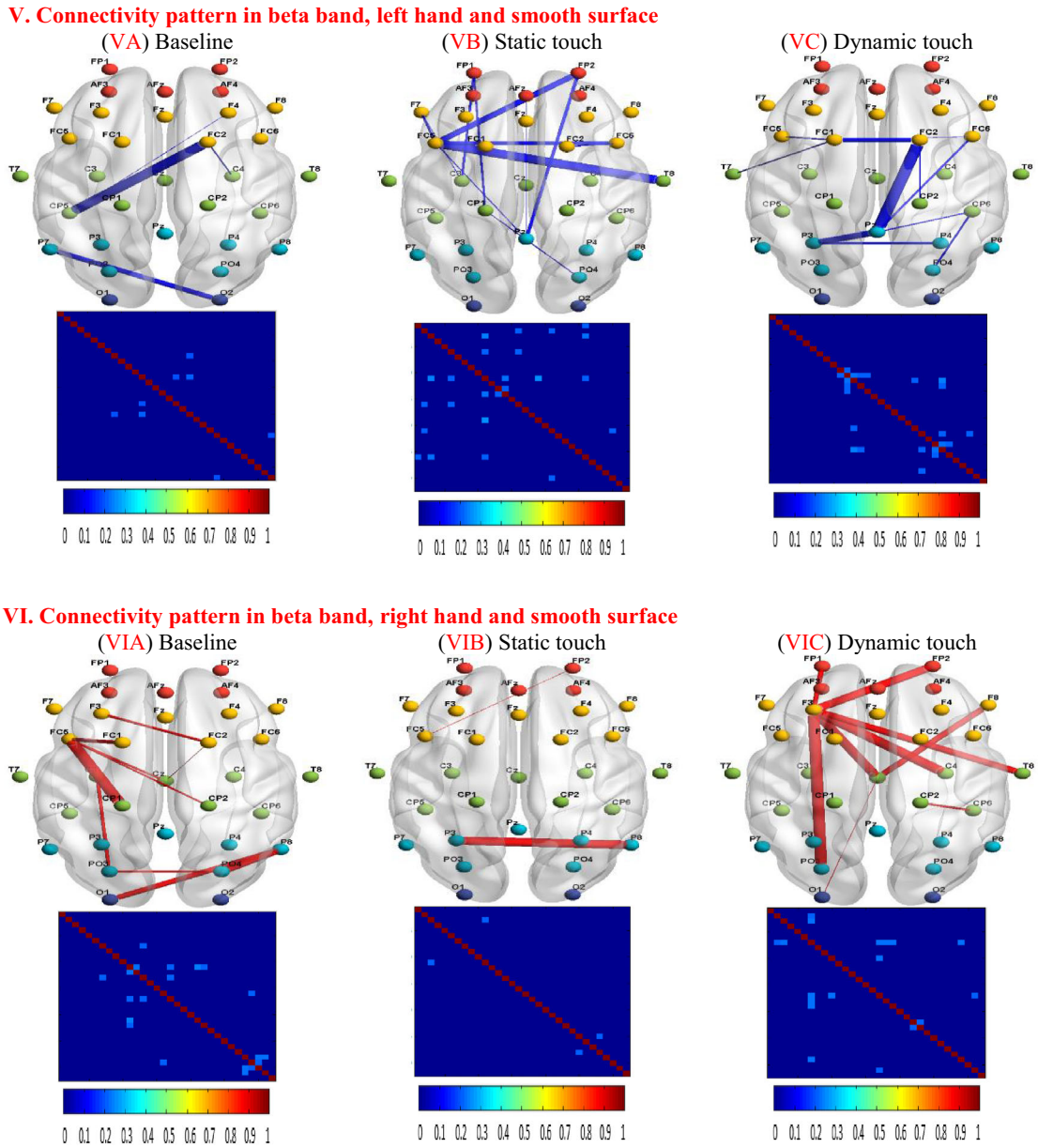

Fig. 5 continued

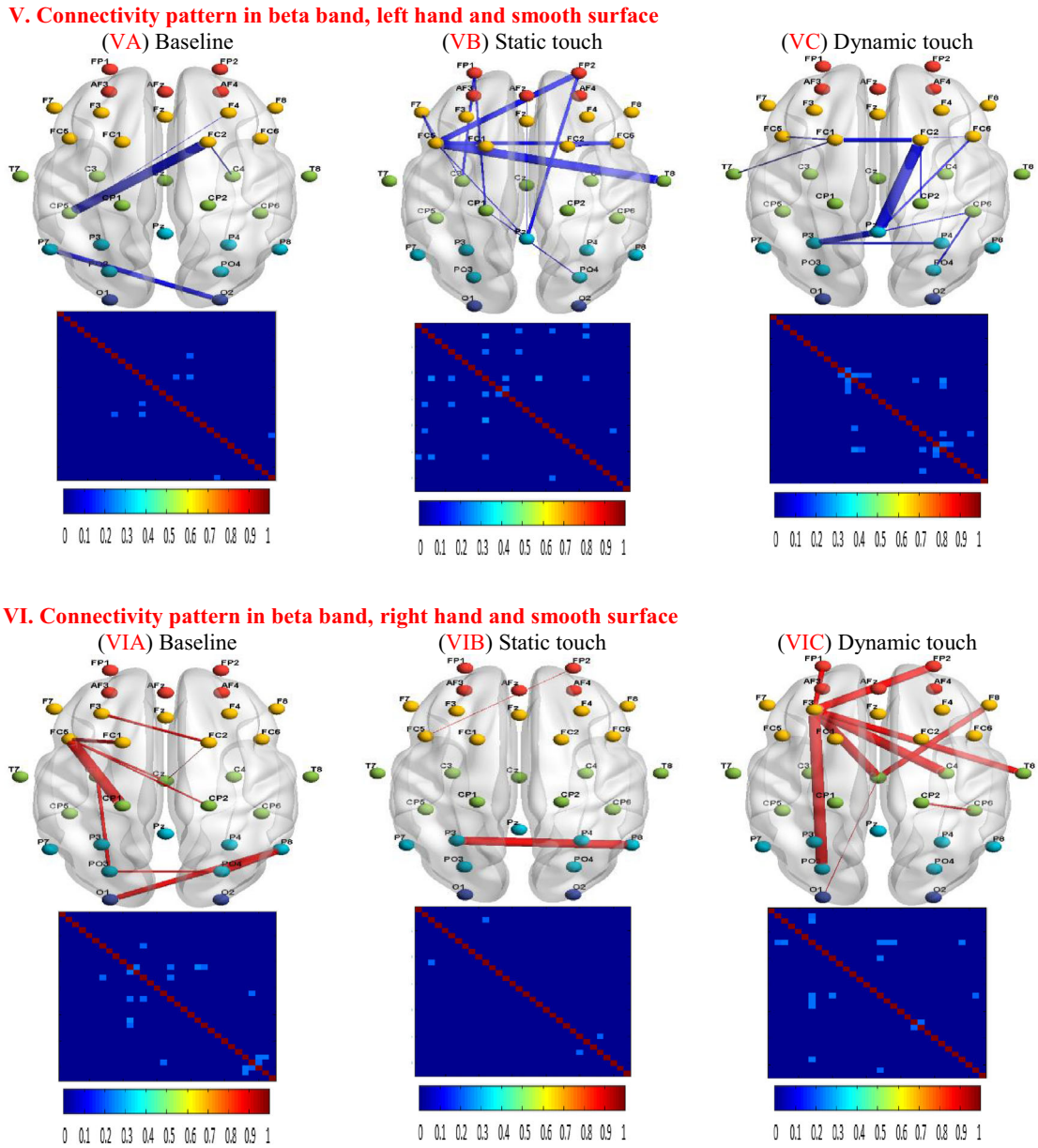

Fig. 5 continued

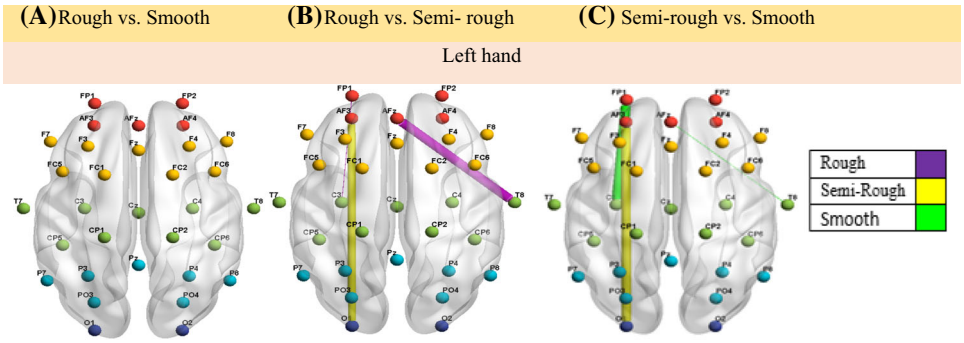

Fig. 6 Significant different (p-value < 0.05) connectivity pattern using the PLI estimator in beta band between the three roughness levels for the left hand in static touch. **A** No significant difference was observed between RS and SS. **B** Significant differences between RS and SRS: the connections in purple indicate that the connections for the RS were stronger than the SRS and the yellow line represents the opposite case. **C** Significant differences between SS and SRS: the connection in yellow indicates that the SRS was stronger than the SS and the green lines represent the opposite case. Note that for the left hand, the significant differences were seen between the RS and the SRS and also SRS and SS surfaces, dominant connections indicate that the connections for LH-SRS were weaker than the other two surfaces in the beta band. SS: smooth surface, SRS: semi-rough surface, RS: rough surface, RH: right hand, LH: left hand. (Color figure online)

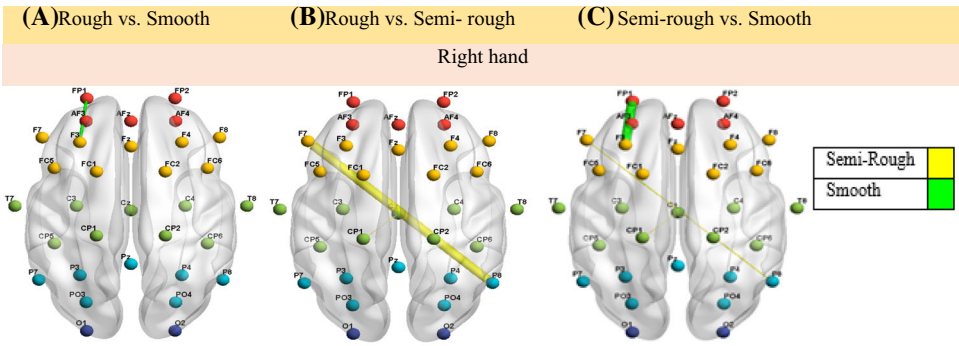

Fig. 7 Significant different (p-value < 0.05) connectivity pattern using the PLI estimator in beta band between the three roughness levels for the right hand in dynamic touch. **A** Significant differences pattern between RS and SS: the connection in green indicates that the connection for SS was stronger than RS. **B** Significant differences between RS and SRS: the connections in yellow indicates that the connection for SRS was stronger than RS. **C** Significant differences between SS and SRS: the connection in yellow indicates that the SRS was stronger than the SS and the green line represents the opposite case. Note that for the right hand, only one significant connection was seen between RS and SS, indicating that the connection for RH-SS is stronger than the RH-RS and in addition, the significant differences were seen between the RS and the SRS and also SRS and SS surfaces, dominant connections indicate that the connections for RH-SRS were stronger than the other two surfaces in the beta band. SS: smooth surface, SRS: semi-rough surface, RS: rough surface, RH: right hand, LH: left hand. (Color figure online)

Table 1 Significant difference in static touch between the right and left hands for each roughness and frequency band

Band \ Surface	Rough	Semi-Rough	Smooth
Delta	✖	Significant difference	✖
Alpha	Significant difference	✖	✖
Beta	✖	Significant difference	Significant difference

Discussion

Tactile sensing is one of the vital senses in the human body and is necessary to interact with the surrounding environment. Associating with the tactile sensation, roughness detection and perception facilities the texture recognition. In this study, we investigated the variation in the pattern of functional connectivity in the brain, when a subject touches surfaces with different levels of roughness. This research was carried out to investigate the variations in connectivity

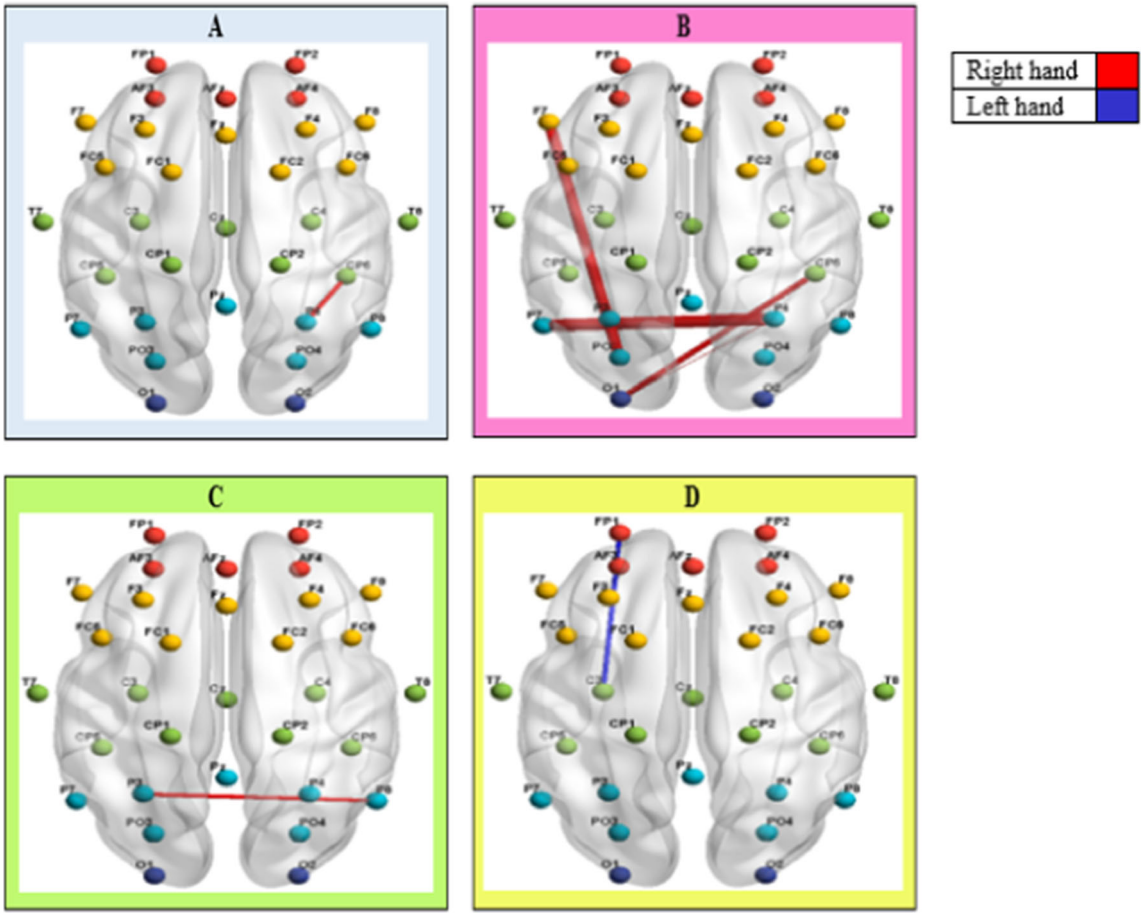

Fig. 8 Significant differences of the PLI values in static touch between the right and left hands. Box **A** Significant differences in delta band connectivity between LH-SRS and RH-SRS: The red line indicates that the connection for the RH-SRS is stronger than the LH-SRS. Box **B** Significant differences in alpha band connectivity between LH-RS and RH-RS: The red lines indicate that the connections for the RH-RS are stronger than the LH-RS. Box **C** Significant differences in beta band connectivity between LH-SRS and RH-SRS: The red line indicates that the connection for the RH-SRS is stronger than the LH-SRS. Box **D** Significant differences in beta band connectivity between LH-SS and RH-SS: The blue line indicates that the connection for the LH-SS is stronger than the RH-SS. SS: smooth surface, SRS: semi-rough surface, RS: rough surface, RH: right hand, LH: left hand. (Color figure online)

Table 2 Significant difference in dynamic touch between the right and left hands for each roughness and frequency band

Band \ Surface	Rough	Semi-Rough	Smooth
Delta	Significant difference	✖	✖
Theta	✖	Significant difference	✖
Alpha	✖	Significant difference	✖

patterns from two points of view: first, the variation in functional connectivity according to tactile stimulation by the dominant and non-dominant hands, and second, the variation in functional connectivity according to experiencing various roughness levels for both hands in static and dynamic touch. In static touch, for the left (non-dominant) hand, we observed a significant connection in alpha band and three significant connections in beta band for both rough versus semi-rough surfaces and semi-rough vs. smooth surfaces. In dynamic touch, for the right (dominant) hand, ten significant connections in alpha band and three significant connections in beta band were observed.

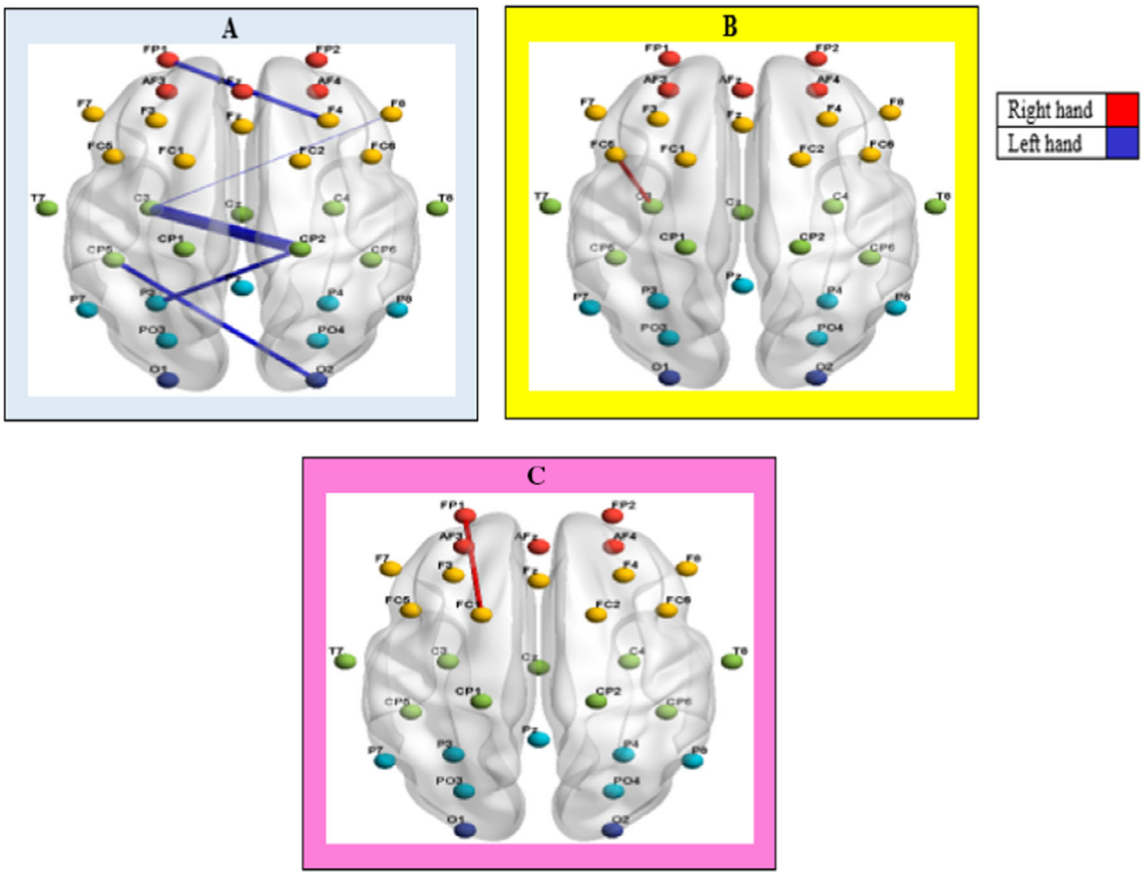

Fig. 9 Significant differences of the PLI values in dynamic touch between the right and left hands. Box **A** Significant differences in delta band connectivity between LH-RS and RH-RS: The blue line indicates that the connection for the LH-RS is stronger than the RH-RS. Box **B** Significant differences in theta band connectivity between LH-SRS and RH-SRS: The red line indicates that the connection for the RH-SRS is stronger than the LH-SRS. Box **C** Significant differences in alpha band connectivity between LH-SRS and RH-SRS: The red line indicates that the connection for the RH-SRS is stronger than the LH-SRS. SS: smooth surface, SRS: semi-rough surface, RS: rough surface, RH: right hand, LH: left hand. (Color figure online)

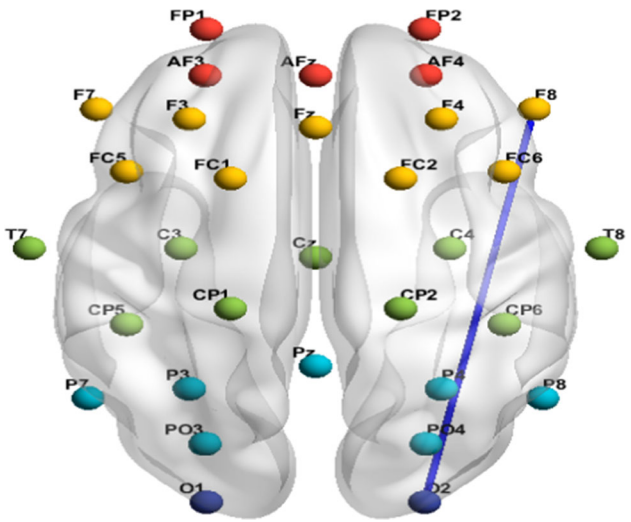

Fig. 10 Connectivity pattern in theta band using the PLI estimator for SRS showing the common connection between all subjects for left hand in static touch. (SRS: semi-rough surface)

Since we observed a significant difference in functional connectivity for static touch only in left hand, the non-dominant hand is probably more sensitive to the roughness levels than the dominant hand in this situation. Furthermore, the right hand showed significant differences in functional connectivity for dynamic touch, hence, the dominant hand is probably more sensitive to the levels of roughness than the non-dominant hand in this case. However, we observed strong connections in all four frequency bands and for all three surface roughness levels. Nevertheless, the significant connections for static touch in delta and beta bands for a semi-rough surface and also in alpha band for a rough surface are stronger for the right hand compared to the left hand. Only a significant connection in beta band was observed for a smooth surface, for which the connection for the left hand was stronger than the right hand. In dynamic touch the significant connections in delta band for a rough surface, for which the connection for the left hand was stronger than the right hand. Moreover, in theta and alpha bands for a semi-rough surface was

Table 3 Common connections in static touch between the right and left hands for each of the roughness levels under the study

Surface Frequency band	Rough	Semi-rough	Smooth
Delta band	No common connection	No common connection	No common connection
Theta band	No common connection	No common connection	No common connection
Alpha band	T8 & C4	F7 & P3–F4 & Fp1	FP1 & AF3–AF4 &F3–F7 & PO3–AF3 & F3–F7 & P8–FP2 & AF3
Beta band	No common connection	No common connection	Fp2 & FC5

Table 4 Common connections in dynamic touch between the right and left hands for each of the roughness levels under the study

Surface Frequency band	Rough	Semi-rough	Smooth
Delta band	No common connection	No common connection	F7 & CP5–F8 & T7
Theta band	Fp1 & FC2–F3 & CP2–FC6 & T7–C3 & CP1–C3 & CP2–FC6 & P8	AFZ & T7–AF3 & T7–F7 & P4–F3 & P3–FC6 & T8–T7 & P8–CP1 & P8–P7 & P4–P3 & PO3	AFZ & T7–AFZ & P4–AFZ &O1–Fp1 & T7–Fp2 & FZ–AF3 & P4–F3 & T7–FC1 & O1–T7 & P4–CP6 & O1–PO4 & O1
Alpha band	No common connection	No common connection	CZ & O2
Beta band	No common connection	No common connection	No common connection

stronger for the right hand compared to the left hand. Moreover, there are common connections between the left and right hands for static touch in alpha band for all three roughness levels and in beta band for the smooth surface and also for dynamic touch in delta band for smooth surface, in theta band for all roughness levels and in alpha band for the smooth surface. Furthermore, the common connections in alpha band for static touch between the two hands decrease by increasing the level of roughness. Also, the common connections in theta band for dynamic touch between the two hands decrease by increasing the level of roughness.

A previous study (Baghdadi et al. 2021) demonstrated that EEG nonlinear characteristics were affected by the alteration of surface roughness and the effects were different between touching by the left or the right hand. Previous research (Ballesteros et al. 2009) related the observed subject's ability to recognize the fine and coarse surfaces, where a coarse surface is easier to discriminate and may evoke an earlier response. Most of the connections in association with the smooth surface are in the frontal and prefrontal regions, where the observed activation could be a result of some level of cognitive-based processing (Genna et al. 2018). A previous work (Genna et al. 2018) demonstrated that event-related desynchronization in alpha band (αERD) undergoes a decreasing trend in both contralateral and ipsilateral hemispheres by increasing the stimulus roughness. It has also been mentioned in previous studies that beta oscillation is associated with attentional and cognitive processes in the brain (Park et al. 2019). Tactile beta oscillations have been proposed to be involved in functional processes within somatosensory cortical areas, in connecting somatosensory regions to parietal and frontal brain regions, and differentiating pleasant from unpleasant touch (Michail et al. 2016). Eldeeb et al. 2020 revealed that spectral EEG features, the total power in the mu (8–15 Hz) and in the beta (16–30 Hz), provide higher accuracy in discriminating textures with different roughness. Furthermore, significant differences in the PSD were observed in beta oscillation in the middle frontal and parietal areas, as well as bilateral parietal areas (Park et al. 2019). The alpha band is activated when a person adapts attention and awareness to distinguish the levels of roughness (Michail et al. 2016). It was also shown in Park and Eid (2018) that in the tactile stimulation mode, the beta power continuously increases and becomes larger than the baseline after about half a second.

Analyzing tactile sensory systems has quite wide applications including the development of electronic skin (Park et al. 2016), BCI systems (Yao et al. 2017), brain stimulation techniques to induce tactile sensing (Collins et al. 2017), and promoting the level of tactile sensitivity (Li et al. 2020). In the present study, we investigated the changes in characteristics of the brain's sensory network when subjects touch surfaces of varying roughness. To gain a better understanding of how the tactile sensory system

works during roughness perception, we calculated the functional connectivity between different brain regions. The results indicate significant differences in static and dynamic touch between rough and semi-rough surfaces, as well as between semi-rough and smooth surfaces. Considering these results, a semi-rough surface may be more suitable for employment in BCI systems. In a previous study (Mao et al. 2021) the linen-stim paradigm resulted in a significant increase in event-related potentials (ERP) compared with the silk-stim paradigm. According to Han et al. (2022), we would make BCIs more flexible with optimizing closed-loop biofeedback systems for internal state detection. Previous studies mainly focused on the appearance and analysis of different brain waves and event-related potentials.

We also observed connections ending up in temporal regions: For the left hand in static and dynamic touch, a functional connection was involved between temporal and other brain regions manifested for the rough surface in delta, theta, and alpha bands, for the semi-rough surface in delta and alpha bands, and for the smooth surface in theta, alpha and beta bands. For the right hand in static and dynamic touch, there was also a functional connection between temporal and other regions for the rough surface in theta, alpha and beta bands, for the semi-rough surface in delta band, and for the smooth surface in theta and alpha bands. Supported by the previous literature, the vibrotactile stimuli can consistently activate the superior temporal gyrus together with the secondary somatosensory cortex (Kim et al. 2015).

This study has some limitations in terms of data acquisition and preprocessing, which require further investigation in the future. A larger sample size and a broad age range are needed to validate the results of current study. Furthermore, the independent component analysis can be performed using EEG automated pre-processing with automatic inspection and rejection of components using either ADJUST and MARA with SASICA or ICLabel (Rodrigues et al. 2021). As discussed in Geller et al. (2014), eye closure can increase the alpha wave. A previous study (Barry et al. 2007) demonstrated that the EEG measures obtained under eyes-closed and eyes-open conditions differ in topography and power levels. In this study, the participants were instructed to close their eyes, so they cannot perceive the roughness of the rotating plate with their visual feedback and a pure tactile perception can be achieved. In the article (Defina et al. 2021), a multivariate and neurodynamic approach has been employed in analysis of EEG modulations induced by touch to highlight differences between patients and healthy controls. It should be noted that in Defina et al. (2021), participants were instructed to close their eyes during the experiment.

Conclusion

In this study, we have investigated the effect of touching three surfaces with different levels of roughness in three situations (baseline, static and dynamic touch) on brain functional connectivity. It has been concluded that the level of roughness affects brain connections. The results have also manifested the functional connectivity in the ipsilateral side of the brain in addition to the contralateral side, and also active connections between the two hemispheres for both hands. Moreover, several strong connections between the two hemispheres were observed. In the end, the functional connectivity involved in differentiating between surfaces in static touch was illustrated only for the left hand and in dynamic touch for the right hand (dominant) in alpha and beta bands. The process explained in this research may open a new window for roughness perception quantification which can be utilized for assessing the effectiveness of the BCI systems in future works.

Supplementary Information The online version contains supplementary material available at https://doi.org/10.1007/s11571-022-09876-1.

Acknowledgements TT and MA would like to thank Mrs. Sahar Dalvand for their valuable assistance in statistical analysis.

Author contributions TT, MRN, MA, and GK did the conception and design, interpretation of results, drafting and revising the article. TT wrote the code for analysis.

Data availability All data are available from the corresponding author upon reasonable request.

Code availability All analyses reported in this work were made with custom code written in MATLAB and will be available from the corresponding author upon reasonable request. Moreover, the last version will be uploaded to GitHub.

Declarations

Conflict of interest The authors declared that they have no competing interests.

References

Afshari S, Jalili M (2016) Directed functional networks in Alzheimer's disease: disruption of global and local connectivity measures. IEEE J Biomed Health Inform 21:949–955

Ala TS, Ahmadi-Pajouh MA, Nasrabadi AM (2018) Cumulative effects of theta binaural beats on brain power and functional connectivity. Biomed Signal Process Control 42:242–252

Astolfi L, Fallani FDV, Cincotti F, Mattia D, Marciani M, Salinari S et al (2008) Estimation of effective and functional cortical connectivity from neuroelectric and hemodynamic recordings. IEEE Trans Neural Syst Rehabil Eng 17:224–233

Baghdadi G, Amiri M, Falotico E, Laschi C (2021) Recurrence quantification analysis of EEG signals for tactile roughness discrimination. Int J Mach Learn Cybern 12:1115–1136

Ballesteros S, Munoz F, Sebastian M, Garcia B, Reales JM (2009) ERP evidence of tactile texture processing: effects of roughness and movement. In: World haptics 2009-third joint EuroHaptics conference and symposium on haptic interfaces for virtual environment and teleoperator systems, IEEE, pp 166–71

Barry RJ, Clarke AR, Johnstone SJ, Magee CA, Rushby JA (2007) EEG differences between eyes-closed and eyes-open resting conditions. Clin Neurophysiol 118:2765–2773

Benjamini Y (2010) Discovering the false discovery rate. J Royal Stat Soc Ser B (Stat Methodol) 72:405–416

Campus C, Brayda L, De Carli F, Chellali R, Famà F, Bruzzo C et al (2012) Tactile exploration of virtual objects for blind and sighted people: the role of beta 1 EEG band in sensory substitution and supramodal mental mapping. J Neurophysiol 107:2713–2729

Chai MT, Saad MNM, Kamel N, Malik AS (2017) EEG analysis of color effects using effective connectivity based on graph theory during a multimedia learning task. In: 2017 IEEE life sciences conference (LSC), IEEE, pp 99–102

Collins KL, Guterstam A, Cronin J, Olson JD, Ehrsson HH, Ojemann JG (2017) Ownership of an artificial limb induced by electrical brain stimulation. Proc Natl Acad Sci 114:166–171

Conte A, Belvisi D, Tartaglia M, Cortese FN, Baione V, Battista E et al (2017) Abnormal temporal coupling of tactile perception and motor action in Parkinson's disease. Front Neurol 8:249

Defina S, Niedernhuber M, Shenker N, Brown CA, Bekinschtein TA (2021) Attentional modulation of neural dynamics in tactile perception of complex regional pain syndrome patients. Eur J Neurosci 54:5601–5619

Delorme A, Makeig S (2004) EEGLAB: an open source toolbox for analysis of single-trial EEG dynamics including independent component analysis. J Neurosci Methods 134:9–21

Ding S, Pan Y, Tong M, Zhao X (2017) Tactile perception of roughness and hardness to discriminate materials by friction-induced vibration. Sensors 17:2748

Eldeeb S, Weber D, Ting J, Demir A, Erdogmus D, Akcakaya M (2020) EEG-based trial-by-trial texture classification during active touch. Sci Rep 10:1–13

Gaetz W, Jurkiewicz MT, Kessler SK, Blaskey L, Schwartz ES, Roberts TP (2017) Neuromagnetic responses to tactile stimulation of the fingers: evidence for reduced cortical inhibition for children with autism spectrum disorder and children with epilepsy. NeuroImage Clin 16:624–33

Geller AS, Burke JF, Sperling MR, Sharan AD, Litt B, Baltuch GH et al (2014) Eye closure causes widespread low-frequency power increase and focal gamma attenuation in the human electrocorticogram. Clin Neurophysiol 125:1764–1773

Genna C, Oddo CM, Fanciullacci C, Chisari C, Jörntell H, Artoni F et al (2017) Spatiotemporal dynamics of the cortical responses induced by a prolonged tactile stimulation of the human fingertips. Brain Topogr 30:473–485

Genna C, Oddo C, Fanciullacci C, Chisari C, Micera S, Artoni F (2018) Bilateral cortical representation of tactile roughness. Brain Res 1699:79–88

Han Y, Ziebell P, Riccio A, Halder S (2022) Two sides of the same coin: adaptation of BCIs to internal states with user-centered design and electrophysiological features. Brain-Comput Interfaces 9:102–114

Hurtado JM, Rubchinsky LL, Sigvardt KA (2004) Statistical method for detection of phase-locking episodes in neural oscillations. J Neurophysiol 91:1883–1898

Jung T-P, Makeig S, Humphries C, Lee T-W, Mckeown MJ, Iragui V et al (2000) Removing electroencephalographic artifacts by blind source separation. Psychophysiology 37:163–178

Kim J, Chung YG, Park J-Y, Chung S-C, Wallraven C, Bülthoff HH et al (2015) Decoding accuracy in supplementary motor cortex correlates with perceptual sensitivity to tactile roughness. PLoS ONE 10:e0129777

King FW (2009) Hilbert transforms, vol 2, Cambridge University Press

Kitada R, Hashimoto T, Kochiyama T, Kito T, Okada T, Matsumura M et al (2005) Tactile estimation of the roughness of gratings yields a graded response in the human brain: an fMRI study. Neuroimage 25:90–100

Lederman SJ, Klatzky RL (2009) Haptic perception: a tutorial. Atten Percept Psychophys 71:1439–1459

Li Q, Kroemer O, Su Z, Veiga FF, Kaboli M, Ritter HJ (2020) A review of tactile information: perception and action through touch. IEEE Trans Rob 36:1619–1634

Liu Y, Bao R, Tao J, Li J, Dong M, Pan C (2020) Recent progress in tactile sensors and their applications in intelligent systems. Science Bulletin 65:70–88

Logozzo S, Valigi MC, Malvezzi M (2022) Modelling the human touch: a basic study for haptic technology. Tribol Int 166:107352

Manfredi LR, Saal HP, Brown KJ, Zielinski MC, Dammann JF III, Polashock VS et al (2014) Natural scenes in tactile texture. J Neurophysiol 111:1792–1802

Mao Y, Jin J, Li S, Miao Y, Cichocki A (2021) Effects of skin friction on tactile P300 brain-computer interface performance. Comput Intell Neurosci 2021 Article ID 6694310, https://doi.org/10.1155/2021/6694310.

Michail G, Dresel C, Witkovský V, Stankewitz A, Schulz E (2016) Neuronal oscillations in various frequency bands differ between pain and touch. Front Hum Neurosci 10:182

Mohan A, De Ridder D, Vanneste S (2016) Graph theoretical analysis of brain connectivity in phantom sound perception. Sci Rep 6:19683

Moscatelli A, Scotto CR, Ernst MO (2019) Illusory changes in the perceived speed of motion derived from proprioception and touch. J Neurophysiol 122: 1555–1565.

Muñoz F, Reales JM, Sebastián MÁ, Ballesteros S (2014) An electrophysiological study of haptic roughness: effects of levels of texture and stimulus uncertainty in the P300. Brain Res 1562:59–68

Natsuko N, Yasushi S, Makoto W, Nobutaka H, Shigeru K (2015) Effects of aging and idiopathic Parkinson's disease on tactile temporal order judgment. PloS ONE 10:e0118331

Oddo CM, Mazzoni A, Spanne A, Enander JM, Mogensen H, Bengtsson F et al (2017) Artificial spatiotemporal touch inputs reveal complementary decoding in neocortical neurons. Sci Rep 7:1–17

Park M, Park YJ, Chen X, Park YK, Kim MS, Ahn JH (2016) MoS2-based tactile sensor for electronic skin applications. Adv Mater 28:2556–2562

Park W, Jamil MH, Eid M (2019) Neural activations associated with friction stimulation on touch-screen devices. Front Neurorobot 13:27

Park W, Eid M (2018) Differences in beta oscillation of the middle frontal cortex with or without tactile stimulation in active touch task. In: international conference on human haptic sensing and touch enabled computer applications, Springer, pp 27–35

Raspopovic S, Capogrosso M, Petrini FM, Bonizzato M, Rigosa J, Di Pino G et al (2014) Restoring natural sensory feedback in real-time bidirectional hand prostheses. Sci Transl Med 6:222rs19

Rodrigues J, Weiß M, Hewig J, Allen JJ (2021) EPOS: EEG processing open-source scripts. Front Neurosci 15:663

Rosenblum MG, Pikovsky AS, Kurths J (1996) Phase synchronization of chaotic oscillators. Phys Rev Lett 76:1804

Rubinov M, Sporns O (2010) Complex network measures of brain connectivity: uses and interpretations. Neuroimage 52:1059–1069

Ryan CP, Bettelani GC, Ciotti S, Parise C, Moscatelli A, Bianchi M (2021) The interaction between motion and texture in the sense of touch. J Neurophysiol 126:1375–1390

Stam CJ, Nolte G, Daffertshofer A (2007) Phase lag index: assessment of functional connectivity from multi channel EEG and MEG with diminished bias from common sources. Hum Brain Mapp 28:1178–1193

Sun J, Hong X, Tong S (2012) Phase synchronization analysis of EEG signals: an evaluation based on surrogate tests. IEEE Trans Biomed Eng 59:2254–2263

Tavassoli T, Bellesheim K, Tommerdahl M, Holden JM, Kolevzon A, Buxbaum JD (2016) Altered tactile processing in children with autism spectrum disorder. Autism Res 9:616–620

Tiwana MI, Redmond SJ, Lovell NH (2012) A review of tactile sensing technologies with applications in biomedical engineering. Sens Actuators A: Phys 179:17–31

Varotto G, Visani E, Canafoglia L, Franceschetti S, Avanzini G, Panzica F (2012) Enhanced frontocentral EEG connectivity in photosensitive generalized epilepsies: a partial directed coherence study. Epilepsia 53:359–367

WM Associaction (2013) World Medical Association Declaration of Helsinki: ethical principles for medical research involving human subjects. JAMA 310:2191–2194

Yao M, Wang R (2019) Neurodynamic analysis of Merkel cell–neurite complex transduction mechanism during tactile sensing. Cogn Neurodyn 13:293–302

Yao L, Sheng X, Mrachacz-Kersting N, Zhu X, Farina D, Jiang N (2017) Decoding covert somatosensory attention by a BCI system calibrated with tactile sensation. IEEE Trans Biomed Eng 65:1689–1695

Yourself MBHIaDI (2013) Table comparing sandpaper grit standard in Europe and USA

Ziebell P, Stümpfig J, Eidel M, Kleih S, Kübler A, Latoschik M et al (2020) Stimulus modality influences session-to-session transfer of training effects in auditory and tactile streaming-based P300 brain–computer interfaces. Sci Rep 10:1–12